

Fractal multi-scale nature of solar/stellar magnetic field

Valentina I. Abramenko

*Big Bear Solar Observatory, New Jersey Institute of Technology, Big Bear City, CA 92314,
USA*

ABSTRACT

An abstract mathematical concept of fractal organization of certain complex objects received significant attention in astrophysics during last decades. The concept evolved into a broad field including multi-fractality and intermittency, percolation theory, self-organized criticality, theory of catastrophes, etc. Such a strong mathematical and physical approach provide new possibilities for exploring various aspects of astrophysics. In particular, in the solar and stellar magnetism, multi-fractal properties of magnetized plasma turned to be useful for understanding burst-like dynamics of energy release events, conditions for turbulent dynamo action, nature of turbulent magnetic diffusivity, and even the dual nature of solar dynamo. In this talk, I will briefly outline how the ideas of multi-fractality are used to explore the above mentioned aspects of solar magnetism.

1. Introduction: Why Fractals?

A mathematical fractal is a self-similar object on all possible spatial and time scales. It means that when we proceed from large to smaller scales, we will see exactly the same picture. From mathematical standpoint this means that a unique scaling law holds for all scales. A fractal (or, more rigorously, a mono-fractal) is a deterministic, predictable system. Mathematical mono-fractals differ drastically from what we observe in nature: fractal-like structures in nature are *multi-fractals* - a superposition of infinite number of mono-fractals.

The transition from mono-fractals to multi-fractals turns an amusing mathematical toy into a powerful tool to study real processes in nature. The matter is that multi-fractals possess the same properties in both the spatial and temporal domains. This means that if we see a very complex, jagged shape in space (multi-fractal in space), then we will observe a violent, burst-like behavior in time (multi-fractal in time). For such systems, any small perturbation can cause an avalanche of any possible size.

Therefore, revealing the fact that a system under study is a fractal does not allow us to make inferences about its nature and essential properties of its behavior. We need something

more, namely, to know of how many mono-fractals our system is made of. Numerous examples of fractals and multi-fractals can be found (e.g., Feder 1989; Schroeder 2000, Internet).

Mathematical details of the fractal calculus are well described as well (e.g., Baumann 2005; McAteer et al. 2007). Historically, when analyzing spatial objects, their capability to be organized into very jagged structures with extended voids and sharp peaks is addressed as a property of multi-fractality. At the same time, while analyzing time series, we address the same property as intermittency. Thus, multi-fractality and intermittency are two terms for the same physical property of a system. I will use both of them in this talk.

Several approaches were elaborated during a couple of last decades to probe the properties of multi-fractality in different fields of science. In a brief review below, I will focus on multi-fractality techniques applied in astrophysics. Thus, multi-fractal systems are capable of self-organization (i.e., formation of larger entities from smaller ones via inverse cascade), and of self-organized criticality (SOC) when burst-like energy release events of any scale are possible at any moment (e.g., Charbonneau et al. 2001; Longcope & Noonan 2000; Aschwanden 2011).

A theory of catastrophes is also based on the multi-fractal nature of astrophysical phenomena (Priest & Forbes 2002; Isenberg & Forbes 2007). Percolating clusters (Balke et al. 1993; Seiden & Wentzel 1996; Pustil'nik 1999; Schatten 2007) are also fractals and multi-fractals.

Direct calculations of fractal dimensions and spectra of multi-fractality is one of the most popular tool to explore astrophysical multi-fractals (e.g., Lawrence et al. 1993; Meunier 1999; Lepreti et al. 1999; McAteer et al. 2007; Dimitropoulou et al. 2009; Abramenko & Yurchyshyn 2010a; Aschwanden 2011).

Another possibility to study multi-fractality is to analyze high statistical moments by means of distribution functions (Bogdan et al. 1988; Parnell et al. 2009), or structure functions (Consolini et al. 1999; Abramenko et al. 2002; Abramenko 2005; Uritsky et al. 2007; Abramenko & Yurchyshyn 2010b; Abramenko et al. 2012).

Essential physical properties of multi-fractals can be formulated as follows.

- (i) Scaling laws change with scale, i.e., no unique power law index can be valid for all scales;
- (ii) Large fluctuations (in both time and space domains) are not rare and contribute significantly to high statistical moments, which grow as the data set expands;
- (iii) Direct and inverse cascades along scales are possible (fragmentation and aggregation), which results in capability to form larger features from smaller ones, i.e., self-organization and SOC state.

These properties can help us to diagnose the presence and degree of multi-fractality of various

astrophysical phenomena. Meanwhile, keeping in mind that in astrophysical magnetism we deal with a specific type of a multi-fractal medium, namely, *intermittent turbulence in an electro-conductive flow*, we can take advantage of it and incorporate other very important properties and tools. So our list of properties can be extended:

(iv) Intermittent turbulent magnetized plasma is capable of amplifying a seed magnetic field, i.e., local fast dynamo is at work (Zeldovich et al. 1987; Biskamp 1993; Vögler & Schüssler 2007; Pietarila Graham et al. 2010), see also a recent review by Brandenburg et al. (2012);

(v) Turbulent plasma at high Reynolds number displays properties of multi-fractality and intermittency in spatial/temporal structures of temperatures, velocities, density, etc. (see, e.g., Zeldovich et al. 1987; Frisch 1995);

(vi) The regime of diffusivity on multi-fractals is expected to be an anomalous diffusion.

Based on these properties of multi-fractal systems, I will discuss below how exploration of these properties can help us in understanding of solar and stellar magnetism. It is impossible in the framework of this invited talk to discuss all aforementioned approaches and tools in great details, so I will concentrate on the analysis of structure functions, which are used in my research.

2. Structure functions approach to study multi-fractality

Since Kolmogorov's study (Kolmogorov 1941), various models have been proposed to describe the statistical behavior of fully developed turbulence. In these studies, the flow is modeled using statistically averaged quantities, and structure functions play a significant role. They are defined as statistical moments of the q -powers of the increment of a field. The definition can be applied to different fields (e.g., velocity, temperature, magnetic field, etc). Here, in the most of the cases, I will refer to the line-of-sight component of the magnetic field, B_l , for which the structure function can be written as

$$S_q(r) = \langle |B_l(\mathbf{x} + \mathbf{r}) - B_l(\mathbf{x})|^q \rangle, \quad (1)$$

where \mathbf{x} is the current pixel on a magnetogram, \mathbf{r} is the separation vector between any two points used to measure the increment (see the lower right panel in Figure 1, and q is the order of a statistical moment, which takes on real values. The angular brackets denote averaging over the magnetogram, and the vector \mathbf{r} is allowed to adopt all possible orientations, θ , on the magnetogram. The next step is to calculate the scaling of the structure functions, which is defined as the slope, $\zeta(q)$, measured inside some range of scales where the $S_q(r)$ -function is linear and the field is intermittent. The function $\zeta(q)$ is shown in the upper right panel in Figure 1.

A weak point in the above technique is the determination of the range, Δr , where the slopes

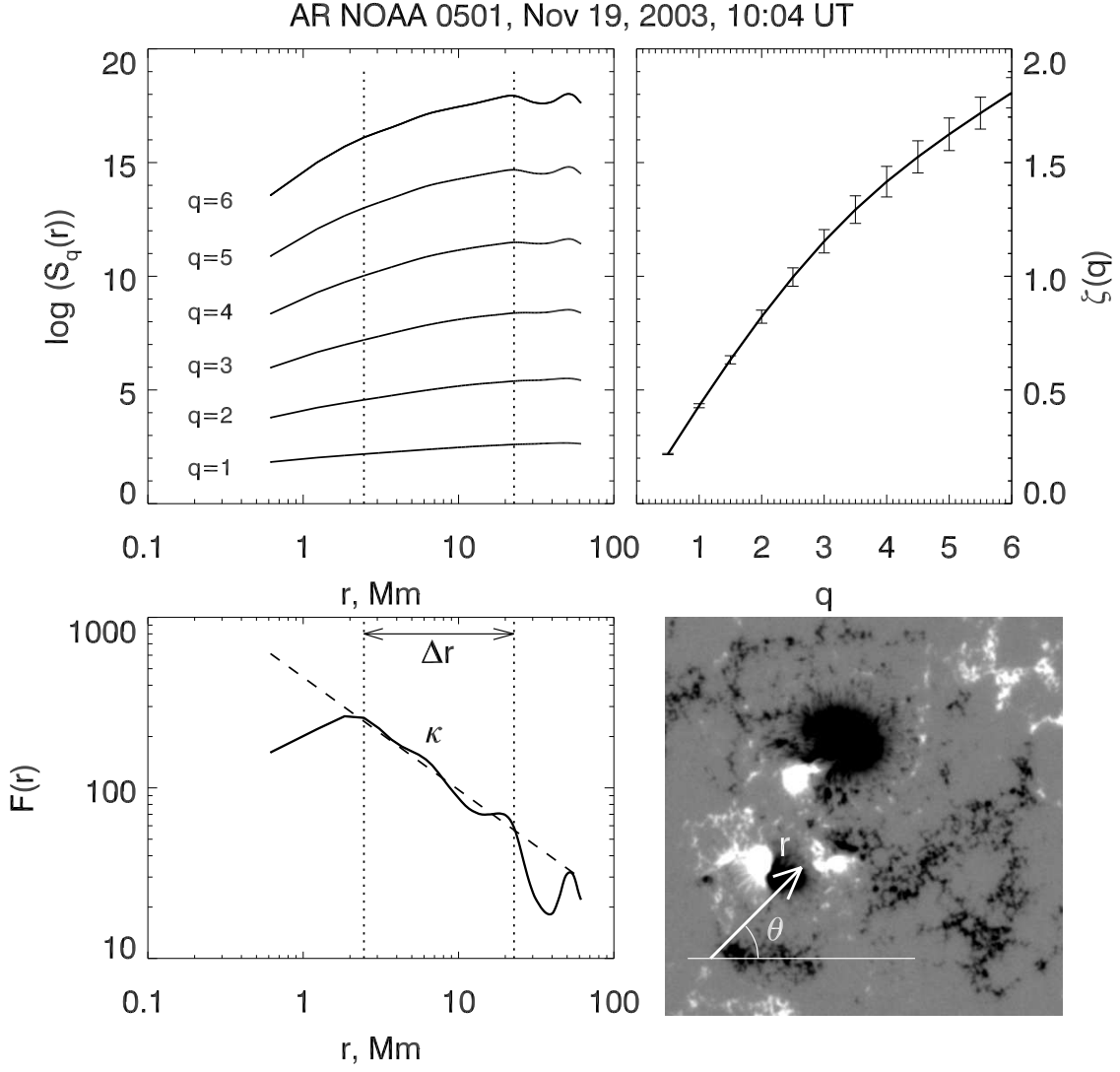


Fig. 1.— Structure functions $S_q(r)$ (*upper left*) calculated from a magnetogram of active region NOAA 0501 (*lower right*) according to Eq. (1). *Lower left* - flatness function $F(r)$ derived from the structure functions using Eq. (2). Vertical dotted lines in both left panels mark the interval of intermittency, Δr , where flatness grows as power law when r decreases. The index κ is the power index of the flatness function determined within Δr . The slopes of $S_q(r)$, defined for each q within Δr , constitute $\zeta(q)$ function (*upper right*), which is concave (straight) for a multi-fractal/intermittent (mono-fractal/non-intermittent) field. An example of a separation vector \mathbf{r} and the corresponding directional angle θ are shown on the magnetogram.

of the structure functions are to be calculated. To visualize the range of intermittency, Δr , we suggest to use the flatness function (Abramenko 2005), which is determined as the ratio of the fourth statistical moment to the square of the second statistical moment. To better identify the effect of intermittency, we reinforced the definition of the flatness function and calculated the hyper-flatness function, namely, the ratio of the sixth moment to the cube of the second moment:

$$F(r) = S_6(r)/(S_2(r))^3 \sim k^{-\kappa}. \quad (2)$$

For simplicity, we will refer to $F(r)$ as the flatness function, or multi-fractality/intermittency spectrum. For a non-intermittent structure, the flatness function is not dependent on the scale, r . On the contrary, for an intermittent/multi-fractal structure, the flatness grows as power-law, when the scale decreases. The slope of flatness function, κ , and the width of Δr characterize the degree of multi-fractality and intermittency.

Application of this technique to two hundred of solar active regions observed with SOHO/MDI in the high resolution mode (Abramenko & Yurchyshyn 2010a) demonstrated that active regions of high flare productivity display steeper and broader multifractality spectra, $F(r)$. The inference agrees with the formulated above statement that multi-fractality in spatial domain is accompanied by intermittency (burst-like behavior) in time. Moreover, for any multi-fractal system, individual bursts cannot be precisely predicted in advance. So, the exact prediction of the location and the onset moment of a flare (of any size), strictly speaking, is a hopeless task. Based on different indirect indications, one may only hope to provide a probabilistic estimate for ongoing flaring.

Multi-fractality of time series of X-ray emission from an individual solar flare was discussed in McAteer et al. (2007), where an inference on the fractal nature of the flaring current sheet was made.

I will focus below on a solar surface outside active regions, which occupy usually more than 80% of the entire solar surface. Many important aspects of solar magnetism are rooted there.

3. Multi-fractality in the solar surface

Examples of line-of-sight (LOS) magnetograms recorded in coronal holes (CHs) using different solar instruments are shown in Figure 2. The left panel shows data from the Helioseismic and Magnetic Imager (HMI) onboard the Solar Dynamics Observatory (SDO, Scherrer et al. 2012), the middle panel shows LOS magnetic field provided by Hinode Solar Optical Telescope Spectro-Polarimeter (SOT/SP, Tsuneta et al. 2008), and the right panel presents a magnetogram from the New Solar Telescope (NST) (Goode et al. 2010) operating at the Big Bear Solar Observatory (BBSO). Note that the NST data were obtained at a near-infrared spectral line (1.56 μm) and

represent the magnetic field in the deep photosphere at depths of about 50 km below the $\tau_{500} = 1$ level. Figure 2 clearly demonstrates that with improved telescope resolution more mixed polarity magnetic elements become visible inside a CH. In spite of the fact that the three magnetograms refer to different CHs, this tendency is well defined.

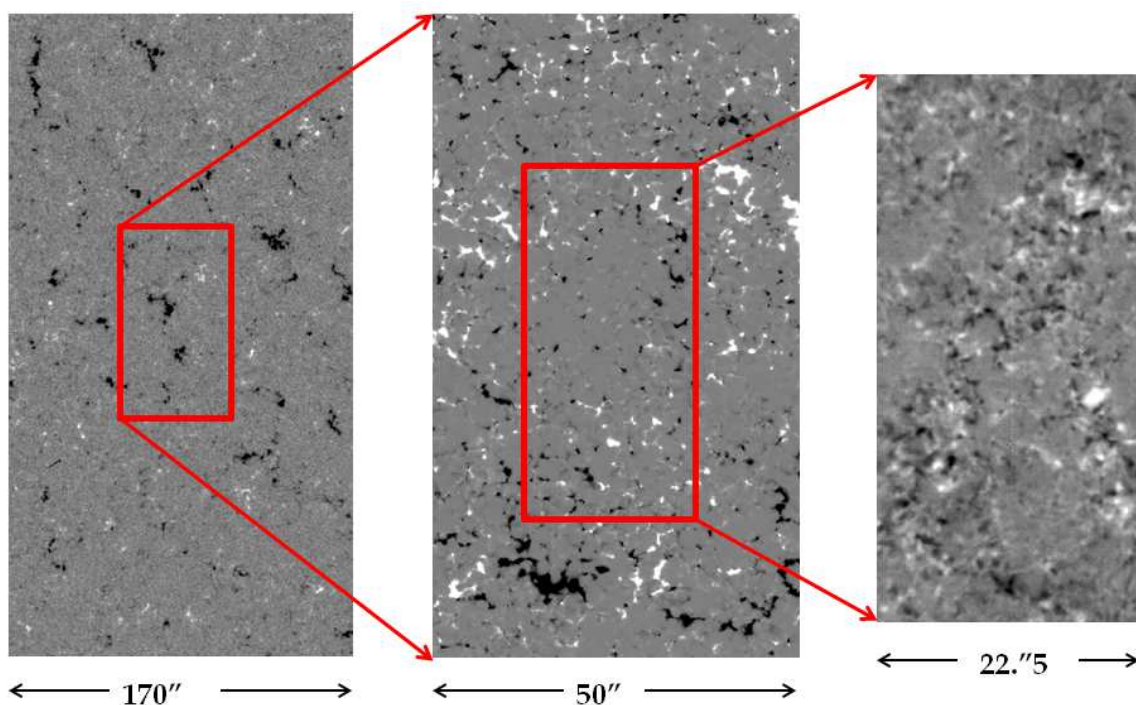


Fig. 2.— Examples of LOS magnetograms recorded inside CHs with three solar instruments (from left to right): SDO/HMI magnetogram (Aug 12, 2011, spatial sampling of 0."5); SOT/SP magnetogram (Mar 10, 2007, spatial sampling of 0."16); BBSO/NST magnetogram (Jun 2, 2012, spatial sampling of 0."098). Red boxes and arrows outline areas of the same size.

Flatness functions calculated from the three above mentioned magnetograms are shown in Figure 3. The HMI data show only a hint of multi-fractality on scales above 1500 km and a very shallow slope of $F(r)$ ($\kappa = -0.07$). The HMI resolution of 1'' obviously is not sufficient to clearly reveal multi-fractality in quiet Sun. Meanwhile, the SOT/SP data show a much broader scale range of multi-fractality down to approximately 630 km and a steeper slope ($\kappa = -0.107$). The HMI result refers to the height of 280-360 km (the effective line formation level of the Fe I 617.3 nm spectral line, Gurtovenko & R.I.Kostyk (1989)), whereas the SOT/NBF data refer to a level of 400-700 km in the photosphere (the line formation height of the Na I 589.6 nm spectral line is discussed in Sheminova (1998)). The flatness function obtained from NST data clearly reveal (at the deeper layer) strong intermittency and multi-fractality on scales down to ~ 400 km.

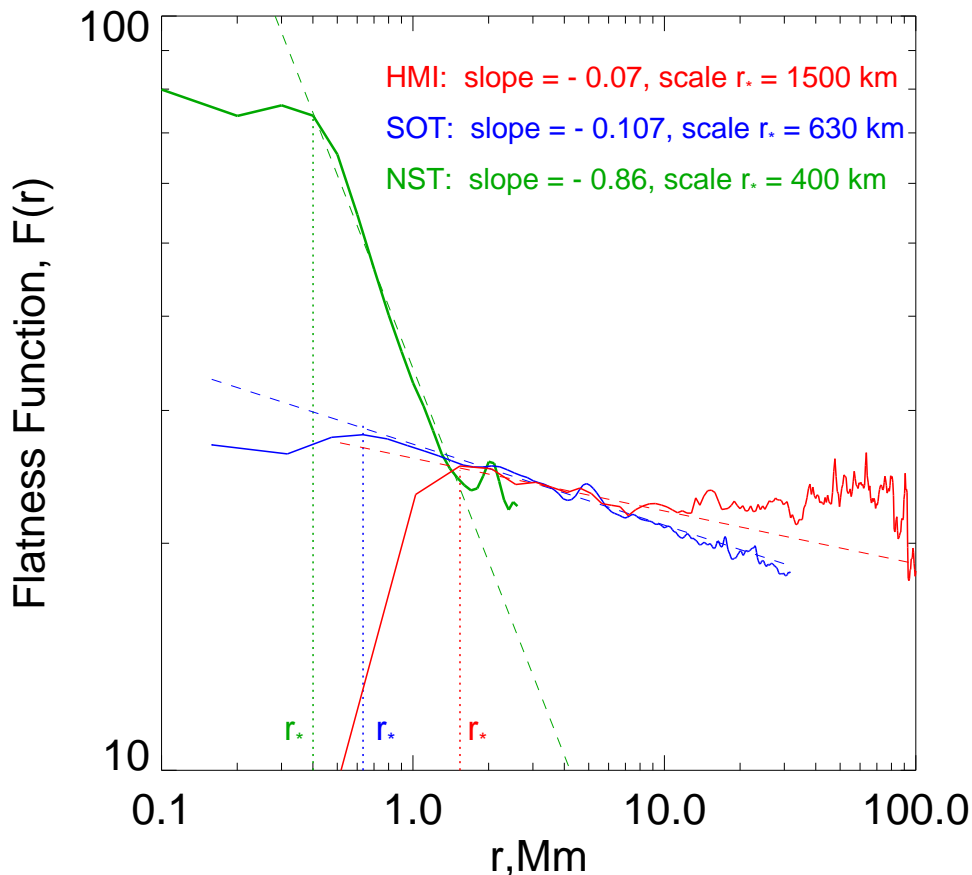


Fig. 3.— Flatness functions calculated from the magnetograms shown in Fig.2. Dashed lines show best linear fits to the data points inside intervals starting above the small-scale cutoff, r_* . For better comparison, the curves are shifted along the vertical axis.

Thus, the multi-fractal nature of small-scale magnetic fields becomes better pronounced with depth and improvement of spatial resolution, which leads us to conclude that intermittency and multi-fractality is an intrinsic property of the near-surface magnetic fields in the quiet Sun.

Magnetic elements against granulation inside a CH are shown in Figure 4, where the background is an NST solar granulation image overplotted with NST LOS and transverse magnetic features and Hinode SOT Narrow Band Filter (NBF) LOS magnetic field.

In the upper right corner of the image, a fragment of bright points (BPs) filigree corresponding to the super-granular boundary is visible. The rest of the image shows the intra-network area, where nine isolated magnetic elements were detected by the SOT/NBF. All of them are co-spatial with BPs and with the LOS signal from the NST. In six cases there are neither opposite polarity nor transverse magnetic field features in the closest vicinity. This may indicate that these mag-

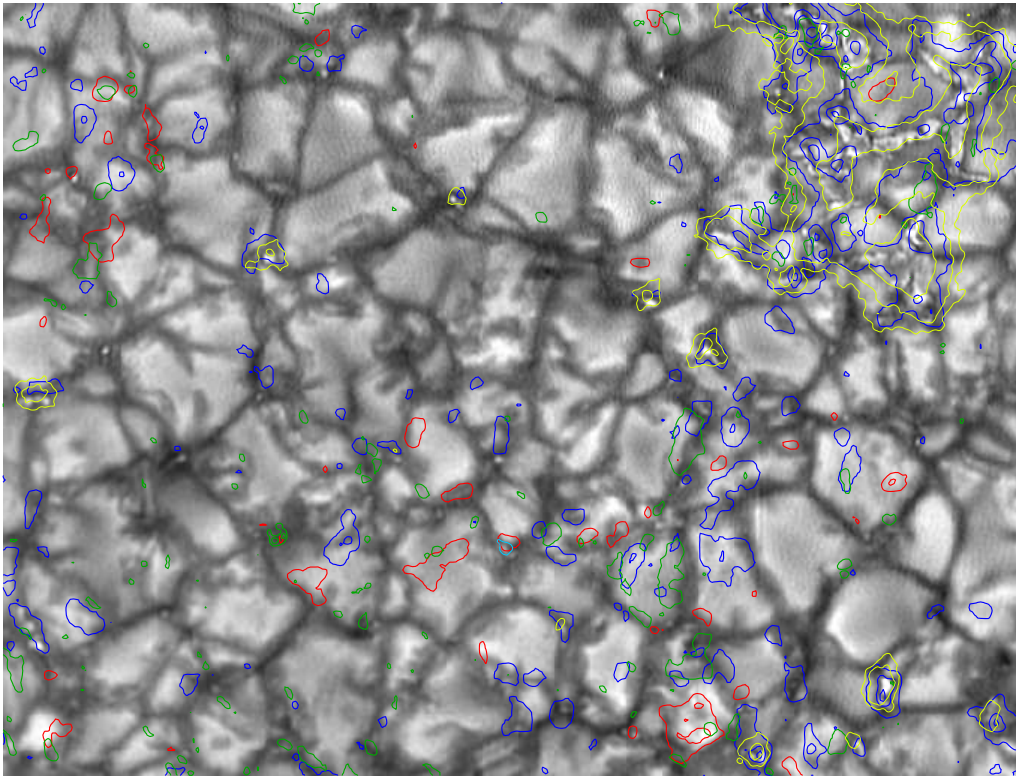


Fig. 4.— Background - NST/TiO image of $26.6''0 \times 20.1''$ in size recorded in a CH at 18:20:32 UT on Aug 12, 2011. Blue (red) contours show the line-of-sight positive (negative) component measured with NST and correspond to 90, 210, 300 G. Green contours represent the signal from the transverse magnetic field component from NST, $(Q^2 + U^2)^{1/2}$, corresponding to 100 and 200 G. Yellow and turquoise contours outline the Hinode SOT/NBF magnetic elements of negative (-50, -100, -300 G) and positive (50 G) polarities for the same day and time.

netic elements are footpoints of open magnetic flux tubes representing the skeleton of the CH. The presence of BPs indicates that they might be produced via the convective collapse (Parker 1978; Spruit 1979).

At the same time, a significant part of the intra-network population is composed of magnetic features, which are not related to BPs and scattered over granules and inter-granular lanes. These magnetic elements were not detected by SOT/NBF and they are not necessarily very weak. On the contrary, they are quite compatible (by size and intensity) with those detected by the both instruments, they are simply not visible in NBF magnetograms. A simplest explanation could be the difference in heights. As I mentioned above, the NST measures the magnetic signal formed very deep in the photosphere, precisely, at the depth of 50 km below the $\tau_{500} = 1$ level, while the

magnetic signal measured with SOT/NBF is formed at the height of approximately 400-700 km. If magnetic elements associated with granules are predominantly small (200-500 km in length) closed loops anchored at a depth of about -50 km, they might not be visible at the altitude of 400-700 km. This speculation is supported by the inspection of mutual location of Stokes V features (blue and red contours) and the transverse magnetic field features (green contours) in Figure 4. Indeed, the V-signal is co-spatial with the $(Q^2 + U^2)$ signal for the granules-associated magnetic elements, which supports the idea of closed loops (or bunches of loops) rather than presence of singular footpoints of extended, high loops or open field lines.

As for the magnetic elements associated with BPs and visible with the both instruments, they seem to be the best candidates for the roots of the open field lines, as we mentioned above. This can explain why they are visible on different heights.

Thus, the data allows us to speculate that the BPs-associated magnetic elements are related to the advection and convective collapse, whereas the numerous granule-associated intra-network elements are situated deeper in the photosphere and might be produced (at least, part of them) by local turbulent dynamo (see the talk by Dr. Tsuneta in this Symposium).

Multi-fractality of granulation. To drive local turbulent dynamo, the environment should be a highly turbulent medium, i.e., to be a multi-fractal. Is the solar granulation pattern a multi-fractal? To explore the question, Abramenko et al. (2012) used a NST data set of solar granulation images obtained for the quiet Sun area on the solar disk center recorded under excellent seeing conditions. Flatness functions for 36 independent snapshots and their average are shown in Figure 5a.

The flatness functions indicate that solar granulation is non-intermittent (a mono-fractal) on scales exceeding approximately 600 km, and it becomes highly intermittent and multi-fractal on scales below 600 km. Thus, a random, Gaussian-like distribution of granule size holds down to 600 km only. On smaller scales, the multi-fractal spatial organization of solar granulation takes over.

A distribution function of granular size (Figure 5b) further confirms this inference. On scales of approximately 600 and 1300 km, the averaged probability distribution function (PDF) rapidly changes its slope. This varying power law PDF is suggestive that the observed ensemble of granules may consist of two populations with distinct properties: regular granules and mini-granules. Decomposition of the observed PDF showed that the best fit is achieved with a combination of a log-normal function, f_1 , representing mini-granules, and a Gaussian function, f_2 , representing regular granules. Their sum perfectly fits to the observational data.

Until now it was thought that solar convection produces convection cells, visible on the solar surface as granules, of characteristic ("dominant") spatial scale of about 1000 km and

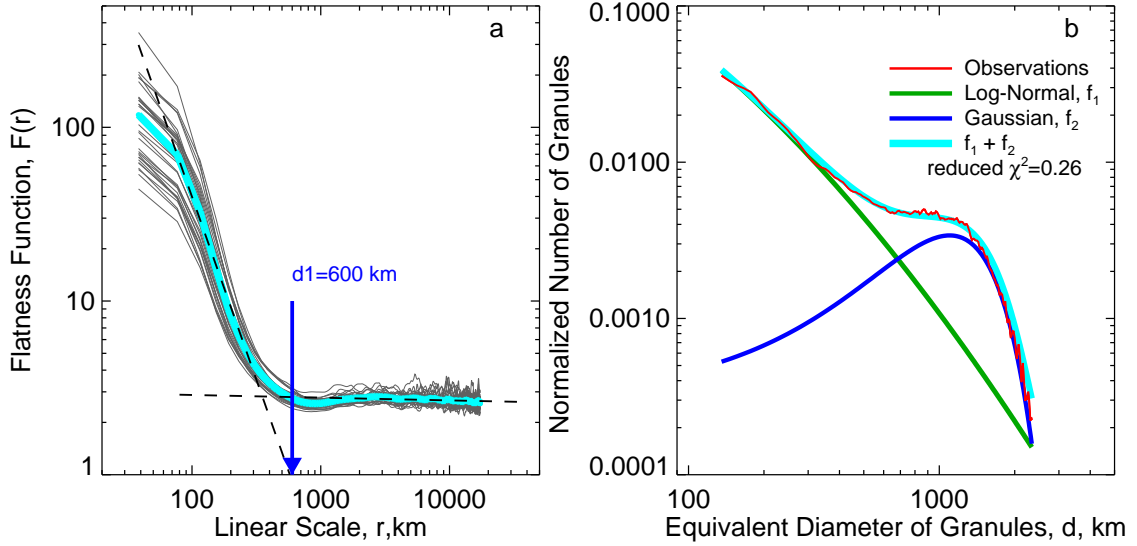


Fig. 5.— *a* - Flatness functions calculated from 36 granulation images (gray) and their average (turquoise). The dashed segments show the best linear fits to the data points. The blue arrow divides the multi-fractality range where the flatness function varies as a power law from the Gaussian range where the flatness function is scale independent. *b* - decomposition of the observed averaged probability distribution function (red line) into two components: a log-normal approximation, (f_1 , green line) and a Gaussian approximation (f_2 , blue). Their sum is plotted with the turquoise line.

a Gaussian (normal) distribution of granule sizes. In this case, the mechanism that produces granules is "programmed" to churn up convection cells of a typical size, without much freedom in size variation. Mini-granules do not display any characteristic ("dominant") scale, their size distribution is continuous and can be described by a decreasing log-normal (Gaussian distribution does not work any longer here). A majority (about 80%) of mini-granules are smaller than 600 km and about 50% are smaller than 300 km in diameter. This non-Gaussian distribution of sizes implies that a much more sophisticated mechanism, with much more degrees of freedom may be at work, where any very small fluctuation in density, pressure, velocity and magnetic fields may have significant impact and affect the resulting dynamics. Physical differences between the log-normal and Gaussian distributions are discussed by, e.g., Abramenko & Longcope (2005).

An important inference from the above discussion reads that a necessary condition for the seed magnetic field to be amplified is met. So, local turbulent dynamo in the near-surface layer is quite a possibility.

Regime of turbulent magnetic diffusion in the photosphere. As we saw in Introduction, the anomalous diffusivity is another hallmark of multi-fractality. The dispersal process embedded

in a multi-fractal cannot follow the random walk with normal diffusion. For example, in the case of solar photosphere, the multi-fractal plasma cannot ensure an arbitrary displacement in an arbitrary direction for all magnetic elements. A discussion of differences between the normal and anomalous diffusion can be found, e.g., in Lawrence & Schrijver (1993); Vlahos et al. (2008).

The coefficient of magnetic diffusivity is an essential input parameter for meridional flux transport models and global dynamo models. Therefore, magnetic flux dispersal on the solar surface was studied extensively (e.g., Lawrence & Schrijver 1993; Schrijver et al. 1996; Berger et al. 1998a,b; Cadavid et al. 1999; Hagenaar et al. 1999; Lawrence et al. 2001; Utz et al. 2009, 2010; Crockett et al. 2010; Abramenko et al. 2011).

In the most of these studies, observational data were interpreted in the framework of normal diffusion, and variety of estimates for the magnetic diffusivity coefficient, η , were reported: from $50 \text{ km}^2\text{s}^{-1}$ (Berger et al. 1998b) to $350 \text{ km}^2 \text{ s}^{-1}$ (Utz et al. 2010). Numerical simulations of the isotropic turbulence with magnetic field (Brandenburg et al. 2008) showed that the turbulent magnetic diffusivity increases with increasing scale. Combination of MHD modeling with observations allowed Chae et al. (2008) to conclude that the turbulent diffusivity changes with scale and is smallest (about $1 \text{ km}^2 \text{ s}^{-1}$) on smallest available scale of approximately 200 km.

Photospheric BPs, as tracers of kilo-gauss magnetic flux tubes, were utilized to probe photospheric flux dispersal (e.g., Berger et al. 1998a,b; Utz et al. 2010; Crockett et al. 2010). Recently, the high resolution power of the NST allowed Abramenko et al. (2011) to explore the regime of diffusion in the photosphere down to scales of 10 sec in time and 25 km in space. Magnetic BPs detected from NST/TiO images were tracked, and their squared displacements (from the initial position of a given BP) were calculated as a function of a time lag, τ . Later, the routine was repeated for HMI magnetic flux concentrations in a quiet Sun area on the disk center. Figure 6a summarizes results.

Recall that for normal diffusion (Brownian motions), the squared displacements of tracers are directly proportional to time, i.e., the power law index, γ , of the displacement spectrum is a unity (an example of the normal diffusion regime is illustrated in Figure 6 with thick black dashed lines). When $\gamma > 1$ ($\gamma < 1$), a regime of super-diffusion (sub-diffusion) dominates. The squared displacements $(\Delta l)^2(\tau)$ can be approximated, at a given range of scales, as

$$(\Delta l)^2(\tau) = c\tau^\gamma, \quad (3)$$

where $c = 10^{y_{sect}}$ and γ and y_{sect} are derived from the best linear fit to the data points plotted in a double-logarithmic plot. Then the diffusion coefficient can be written as (Abramenko et al. 2011):

$$\eta(\tau) = \frac{c\gamma}{4}\tau^{\gamma-1}, \quad (4)$$

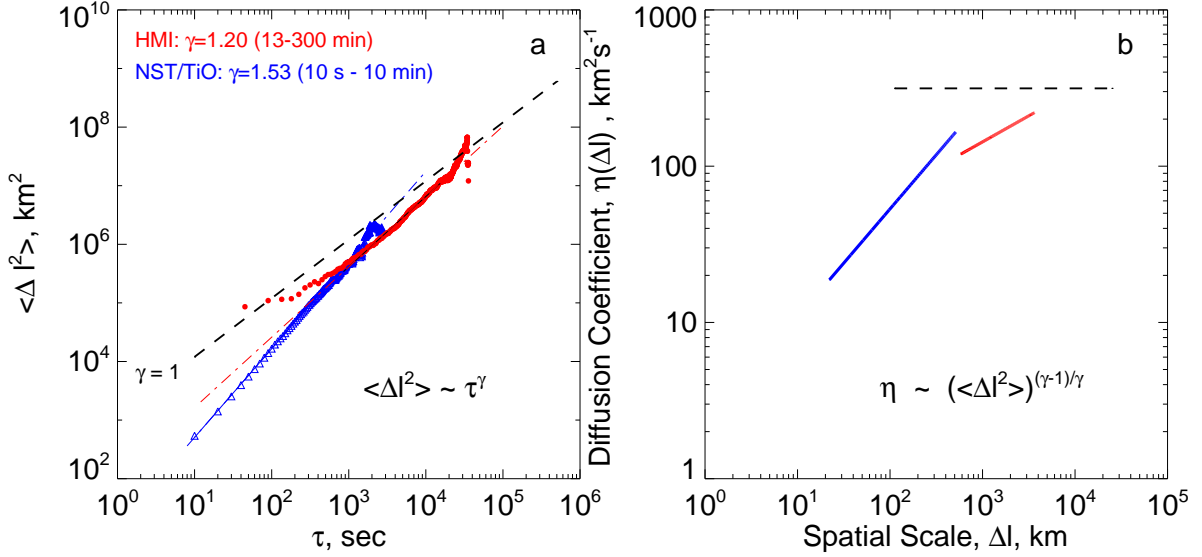


Fig. 6.— *a* - Squared displacements of magnetic BPs detected from a 2-hour data set from the NST/BBSO (*blue*) and squared displacements of magnetic elements detected from 9-hour data set from SDO/HMI magnetograms recorded in a quiet Sun area on the solar disk center (*red*). Dash-dot lines are the best linear fit to the data points inside ranges of linearity; the slopes of the fits, γ , are indicated. *b* - The turbulent magnetic diffusivity, η , as a function of linear scale derived by Eq. (5) from linear fits for the NST (*blue*) and HMI (*red*) data shown in panel *a*. The thick dashed lines in both panels show an example of scaling for the normal diffusion regime with $\gamma = 1$.

$$\eta(\Delta l) = \frac{c^\gamma}{4} ((\Delta l)^2/c)^{(\gamma-1)/\gamma}. \quad (5)$$

As it follows from Figure 6, for both data sets we observe the super-diffusion regime. The coefficient of magnetic turbulent diffusivity, $\eta(\Delta l)$, derived by Eq. (5) for both data sets is shown in Figure 6*b*. Two essential things should be mentioned here: first, the diffusion coefficient grows as the scale increases (the same is true for a time scale, too, see Eq. (4)). Second, the slope of the power law varies with scale (which is a characteristic feature of intrinsic multi-fractality). On the minimal spatial (25 km) and temporal (10 sec) scales considered in Abramenko et al. (2011), the diffusion coefficient in QS area was found to be $19 \text{ km}^2 \text{ s}^{-1}$. The HMI data provided a value of approximately $220 \text{ km}^2 \text{ s}^{-1}$ on the largest available scale of 4 Mm.

The observed tendency of the turbulent magnetic diffusivity to decrease with decreasing scales leads us to expect that the turbulent diffusivity might be close to the magnitudes of diffusivity adopted in the numerical simulations of small-scale dynamo ($0.01 - 10 \text{ km}^2 \text{ s}^{-1}$, e.g., Boldyrev & Cattaneo (2004); Vögler & Schüssler (2007); Pietarila Graham et al. (2010)). This

makes the simulations even more realistic.

In summary, a super-diffusion regime on very small scales is very favorable for pictures assuming turbulent dynamo action since it assumes decreasing diffusivity with decreasing scales.

4. Concluding remarks

Continuously varying magnetic fields are the main reason for the solar/stellar activity. The 11-year solar cycle is one of the most astonishing and widely known examples of the self-organized generation of the magnetic field. Although we know that there is no two absolutely similar solar cycles, yet, persistency and regularity of the solar periodicity through thousands of years remains impressive. A drastically different picture arises when one looks on the photosphere: chaos of mixed-polarity magnetic elements of all sizes until the resolution limits of modern instruments, continuously renewing during 1-2 days - the magnetic carpet.

Dualism of the solar magnetism is usually explained by a simultaneous action of two dynamos: a global dynamo operating in the convective zone and responsible for the 11-year solar cycle, and local, or turbulent dynamo, which might operate inside the near-surface layer and to be responsible for generation of small-scale magnetic fields forming the magnetic carpet. The explanation seems to oversimplify the reality because recent studies of distribution of the magnetic flux accumulated in magnetic flux tubes showed the non-interrupted power law for many decades (Parnell et al. 2009) thus supposing a common (for all scales) mechanism for the magnetic field generation. One of promising ways to handle the problem is to consider the solar dynamo process as a non-linear dynamical system (NDS), with intrinsic properties of multi-fractality and intermittency.

Like any NDS, the solar dynamo is then capable to self-organization on all scales (including large scales) and display a chaotic nature on small scales. Self-organization, in turn, provides for a magnetic complex a way to reach a SOC state, when burst-like energy release events of any size are possible at any time instant. The concept is very important for our understanding of flaring and heating processes in solar/stellar atmospheres.

Further, multi-fractal nature on the magnetic field provides a necessary condition for the local turbulent dynamo operation in the near-surface layer of the convective zone. Observational evidences for local dynamo operation are still under strong debates, e.g., compare the talks by Drs. Tsuneta and Stenflo presented at this symposium.

One pragmatic advise for researchers could be inferred from the observed multi-fractal nature of magnetized solar plasma. Namely, observed power laws should not be extrapolated over neighboring scales, a frequent mistake for power laws studies in various fields.

In summary, the paradigm of multi-fractal and highly intermittent structure of solar magnetized plasma offers new approaches to understand the solar and stellar magnetism.

REFERENCES

- Abramenko, V., & Yurchyshyn, V. 2010a, *ApJ*, 722, 122
- . 2010b, *ApJ*, 722, 122
- Abramenko, V. I. 2005, *Sol. Phys.*, 228, 29
- Abramenko, V. I., Carbone, V., Yurchyshyn, V., Goode, P. R., Stein, R. F., Lepreti, F., Capparelli, V., & Vecchio, A. 2011, *ApJ*, 743, 133
- Abramenko, V. I., & Longcope, D. W. 2005, *ApJ*, 619, 1160
- Abramenko, V. I., Yurchyshyn, V. B., Goode, P. R., Kitiashvili, I. N., & Kosovichev, A. G. 2012, *ApJ*, 756, L27
- Abramenko, V. I., Yurchyshyn, V. B., Wang, H., Spirock, T. J., & Goode, P. R. 2002, *ApJ*, 577, 487
- Aschwanden, M. 2011, *Self-Organized Criticality in Astrophysics - The Statistics of Nonlinear Processes in the Universe*, 1st edn. (Heidelberg Dordrecht London New York: Springer)
- Aschwanden, M. J. 2011, *Sol. Phys.*, 274, 99
- Balke, A. C., Schrijver, C. J., Zwaan, C., & Tarbell, T. D. 1993, *Sol. Phys.*, 143, 215
- Baumann. 2005, *Mathematica for Teoretical Physics* (New York: New York: Springer)
- Berger, T. E., Loefdahl, M. G., Shine, R. S., & Title, A. M. 1998a, *ApJ*, 495, 973
- Berger, T. E., Löfdahl, M. G., Shine, R. A., & Title, A. M. 1998b, *ApJ*, 506, 439
- Biskamp, D. 1993, *Nonlinear Magnetohydrodynamics*, ed. W. Grossman, D. Papadopoulos, R. Sagdeev, & K. Schlindler (Cabmridge, New York, Melbourne: Cambridge University Press)
- Bogdan, T. J., Gilman, P. A., Lerche, I., & Howard, R. 1988, *ApJ*, 327, 451
- Boldyrev, S., & Cattaneo, F. 2004, *Physical Review Letters*, 92, 144501

- Brandenburg, A., Rädler, K.-H., & Schrunner, M. 2008, *âp*, 482, 739
- Brandenburg, A., Sokoloff, D., & Subramanian, K. 2012, *Br*, 169, 123
- Cadavid, A. C., Lawrence, J. K., & Ruzmaikin, A. A. 1999, *ApJ*, 521, 844
- Chae, J., Litvinenko, Y. E., & Sakurai, T. 2008, *ApJ*, 683, 1153
- Charbonneau, P., McIntosh, S. W., Liu, H.-L., & Bogdan, T. J. 2001, *Sol. Phys.*, 203, 321
- Consolini, G., et al. 1999, *âp*, 344, L33
- Crockett, P. J., Mathioudakis, M., Jess, D. B., Shelyag, S., Keenan, F. P., & Christian, D. J. 2010, *ApJ*, 722, L188
- Dimitropoulou, M., Georgoulis, M., Isliker, H., Vlahos, L., Anastasiadis, A., Strintzi, D., & Moussas, X. 2009, *âp*, 505, 1245
- Feder, J. 1989, *Fractals* (New York and London: Plenum Press)
- Frisch, U. 1995, *Turbulence, The Legacy of A.N.Kolmogorov* (Cambridge: Cambridge University Press)
- Goode, P. R., Coulter, R., Gorceix, N., Yurchyshyn, V., & Cao, W. 2010, *Astronomische Nachrichten*, 331, 620
- Gurtovenko, E. A., & R.I.Kostyk. 1989, *Fraunhofer Spectrum* (Kyiv, Ukraine: Naukova Dumka)
- Hagenaar, H. J., Schrijver, C. J., Title, A. M., & Shine, R. A. 1999, *ApJ*, 511, 932
- Isenberg, P. A., & Forbes, T. G. 2007, *ApJ*, 670, 1453
- Kolmogorov, A. 1941, *Akademiia Nauk SSSR Doklady*, 30, 301
- Lawrence, J. K., Cadavid, A. C., Ruzmaikin, A., & Berger, T. E. 2001, *Physical Review Letters*, 86, 5894
- Lawrence, J. K., Ruzmaikin, A. A., & Cadavid, A. C. 1993, *ApJ*, 417, 805
- Lawrence, J. K., & Schrijver, C. J. 1993, *ApJ*, 411, 402
- Lepreti, F., et al. 1999, in *ESA Special Publication, Vol. 448, Magnetic Fields and Solar Processes*, ed. A. Wilson & et al., 327
- Longcope, D. W., & Noonan, E. J. 2000, *ApJ*, 542, 1088

- McAteer, R. T. J., Young, C. A., Ireland, J., & Gallagher, P. T. 2007, *ApJ*, 662, 691
- Meunier, N. 1999, *ApJ*, 527, 967
- Parker, E. N. 1978, *ApJ*, 221, 368
- Parnell, C. E., DeForest, C. E., Hagenaar, H. J., Johnston, B. A., Lamb, D. A., & Welsch, B. T. 2009, *ApJ*, 698, 75
- Pietarila Graham, J., Cameron, R., & Schüssler, M. 2010, *ApJ*, 714, 1606
- Priest, E. R., & Forbes, T. G. 2002, *âpr*, 10, 313
- Pustil'nik, L. A. 1999, *Ap&SS*, 264, 171
- Schatten, K. H. 2007, *ApJS*, 169, 137
- Scherrer, P. H., et al. 2012, *Sol. Phys.*, 275, 207
- Schrijver, C. J., et al. 1996, *ApJ*, 468, 921
- Schroeder, M. 2000, *Fractals, Chaos, Power Laws: Minutes from an Infinite Paradise* (New York: W.H.Freeman and Company)
- Seiden, P. E., & Wentzel, D. G. 1996, *ApJ*, 460, 522
- Sheminova, V. A. 1998, *âp*, 329, 721
- Spruit, H. C. 1979, *Sol. Phys.*, 61, 363
- Tsuneta, S., et al. 2008, *Sol. Phys.*, 249, 167
- Uritsky, V. M., Paczuski, M., Davila, J. M., & Jones, S. I. 2007, *Physical Review Letters*, 99, 025001
- Utz, D., Hanslmeier, A., Möstl, C., Muller, R., Veronig, A., & Muthsam, H. 2009, *A&A*, 498, 289
- Utz, D., Hanslmeier, A., Muller, R., Veronig, A., Rybák, J., & Muthsam, H. 2010, *A&A*, 511, A39+
- Vlahos, L., Isliker, H., Kominis, Y., & Hizanidis, K. 2008, *ArXiv e-prints*
- Vögler, A., & Schüssler, M. 2007, *A&A*, 465, L43

Zeldovich, Y. B., Molchanov, S. A., Ruzmaikin, A. A., & Sokoloff, D. D. 1987, *Sov. Phys. Usp.*,
30, 353